Analytic solutions for the circadian oscillator characterize cycle dynamics and its robustness

Odile Burckard, Madalena Chaves

Analytic solutions for the circadian oscillator characterize cycle dynamics and its robustness

Odile Burckard[1*] and Madalena Chaves[1]

[1*]Centre Inria d'Université Côte d'Azur, INRAE, CNRS, Macbes team, Sophia Antipolis, France .

*Corresponding author(s). E-mail(s): odile.burckard@inria.fr;
Contributing authors: madalena.chaves@inria.fr;

Abstract

Circadian clocks form a fundamental mechanism that promotes the correct behavior of many cellular and molecular processes by synchronizing them on a 24 hour period. However, the circadian cycles remain difficult to describe mathematically. To overcome this problem, we first propose a segmentation of the circadian cycle into eight stages based on the levels of expression of the core clock components CLOCK:BMAL1, REV-ERB and PER:CRY. This cycle segmentation is next characterized through a piecewise linear model, whose analytical study allows us to propose an Algorithm to generate biologically-consistent circadian oscillators. Our study provides a characterization of the cycle dynamics in terms of four fundamental threshold parameters and one scaling parameter, shows robustness of the circadian system and its period, and identifies critical points for correct cycle progression.

Keywords: Circadian clock cycle dynamics, piecewise linear model, analytic solutions, parameter regions, period robustness

1 Introduction

In mammals, every cell contains its own circadian clock network, a complex family of interactions between genes and proteins that helps to control and synchronize many cellular and molecular processes (such as heart beat, blood pressure, body temperature,...). The main synchronizer of circadian clock is known to be the Earth's light/dark cycle, forcing circadian clock period at around 24h. The core mechanism of

circadian clock is based on two negative feedback loops, between the complexes of protein PER:CRY and CLOCK:BMAL1 and between CLOCK:BMAL1 and REV-ERB, allowing circadian clocks to show sustainable and rhythmic oscillations [1, 2] . These interactions between proteins imply a phase opposition between CLOCK:BMAL1 and PER:CRY and a specific order of protein peaks: CLOCK:BMAL1, REV-ERB and PER:CRY. Throughout the years, several mathematical models have been developed, especially for the clock located in the Suprachiasmatic Nucleus (SCN) [3, 4] but also for peripheral organs such as the liver [5–7], or pancreatic beta-cells [8] or for more 'generic'-type cells [2, 9], focusing on different circadian clock features (such as transcription, translation, import/export, degradation, phosphorylation...) and recovering important biological properties of circadian clocks. These models enable, among other points, to provide insights to show circadian period and oscillations robustness whether by studying it with a reduced number of clock molecules (mRNA or proteins) in the cell [10] or demonstrating the role of the two loops [4].

In this paper, we propose a characterization of the circadian cycle based on a segmentation of the circadian time into eight different stages depending on the levels of expression of the three core components CLOCK:BMAL1, REV-ERB and PER:CRY. We construct a piecewise linear differential model which describes the dynamics of the circadian clock in each of these stages. This model leads to analytical solutions that help us to represent the mechanisms of circadian clocks and provide a quantitative method to study the cycle dynamics. Using these analytical solutions, we implement an Algorithm to estimate and explore the parameter space of this cycle segmentation. Our results show that the circadian system is robust in the sense that a periodic orbit with period near 24 hours is observed for a large range of concentrations. This robustness is determined by an adjustment between the minimal concentration of PER:CRY and the maximal concentration of CLOCK:BMAL1: the product of these two quantities may range over a large interval and sets a scaling for the other variables in the system.

2 Numerical and mathematical characterization of circadian time

2.1 A model reproducing circadian clock properties

Throughout this paper, we base our analysis on the continuous circadian clock model recently developed by Almeida et al. [11] . This model, calibrated with data from mouse fibroblast cells [12], focuses on the transcriptional details and describes the dynamics of the core clock protein complexes CLOCK:BMAL1, DBP, REV-ERB (representing both REV-ERBα and REV-ERBβ) and PER:CRY (complex formed by PER2 and CRY1). The proteins are respectively denoted B, D, R and P throughout this paper. The ordinary differential equations of this model are:

$$\begin{aligned} \dot{B} &= V_R h^-(R) - \gamma_B BP, \\ \dot{D} &= V_B B - \gamma_D D, \\ \dot{R} &= V_D D - \gamma_R R, \\ \dot{P} &= V_D D - \gamma_B BP, \end{aligned} \tag{1}$$

where $h^-(R) = \frac{k_{Rr}^4}{k_{Rr}^4+R^4}, V_R = 44.4\%.h^{-1}, k_{Rr} = 80.1\%, V_B = 0.142\%.h^{-1}, V_D = 19\%.h^{-1}, \gamma_R = 0.241h^{-1}, \gamma_D = 0.156h^{-1}, \gamma_B = 2.58h^{-1}$. V_B, V_D and V_R stand for synthesis rates and γ_B, γ_D and γ_R for degradation rates.

2.2 A segmentation of the circadian time into eight stages

We suggest a segmentation of the circadian time into stages based on the repression of CLOCK:BMAL1 by REV-ERB (represented by the term $V_R h^-(R)$ in model 1) and on the dynamics between CLOCK:BMAL1 and PER:CRY (represented by the mutual repression term $\gamma_B BP$ in model 1). We define the different regions by setting thresholds on the variables B, P and R in order to segment the circadian cycle and characterize the clock proteins dynamics. Throughout this paper, we will use "stage i" to designate the time interval spent by a circadian cycle in "region i" of the state space. By abuse of notation, we will use "stage i" to designate both the time interval and (as a label of) "region i".

Let's define P_{low}, a low level of reference for the variable P, B_{high} and P_{high}, high levels of reference for the variables B and P and R_{int} an intermediate level of reference for R. The state space can be partitioned using all the different combinations of the thresholds: as there are two thresholds for P, one for R and one for B, the state space can be divided into twelve stages (see Table 1).

However, as the circadian clock performs one cycle, the phase opposition property between CLOCK:BMAL1 and PER:CRY has to be respected [13], refuting some stages. This property implies that the oscillator cannot have $B < B_{high}$ and $P < P_{low}$ simultaneously (eliminating stages 9 and 10) nor $B > B_{high}$ and $P > P_{high}$ simultaneously (eliminating stages 11 and 12). The circadian cycle is then described by the first eight stages of Table 1.

2.3 Temporal sequence of the stages

The circadian clock shows a specific order of protein peaks: BMAL1 then REV-ERB, then PER:CRY peaks. This property suggests a specific order among stages followed by any circadian oscillator. Notice that the probability that two variables cross their thresholds simultaneously is very small. So, from one stage to another, we assume that only one variable crosses a threshold. It's therefore not possible to pass from stage 1 to 3 for example. We define the peak of B such that B is above its threshold B_{high}, corresponding to stages 5, 6, 7 and 8. The peak of R follows the peak of B and is defined such that R is above R_{int} which is represented by stages 7, 8, 1 and 2. Finally, the peak of P follows the peak of R and corresponds to stages 2 and 3, as $P > P_{high}$. A cycle that respects physiological properties (such as the order of protein peaks) should follow an ascending order of stages and should not enter twice a same stage in a same cycle. The ideal order of stages would then be 1-2-3-4-5-6-7-8-1, as represented in Figure 1. Each stage is represented by a vertex in the space (R, B, P) and is defined via the thresholds R_{int}, B_{high}, P_{low} and P_{high}. The unlabelled vertices correspond to the discarded stages. The ideal order of stages as the circadian oscillator performs one cycle is represented as a transition graph (green arrows) among the eight vertices.

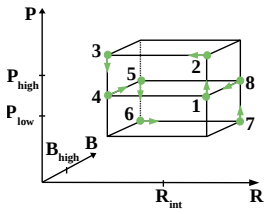

Fig. 1 Ideal physiological order of stages followed by an oscillator as it performs one cycle

3 A piecewise linear clock model

Inspired by the piecewise linear model suggested before by our group [14] and based on the repression of CLOCK:BMAL1 by PER:CRY, on the dynamics between REV-ERB and CLOCK:BMAL1 and on the circadian time decomposition into eight stages, we simplified the continuous model of Almeida et al. (1) into a piecewise linear one, in order to describe the dynamic of the circadian clock in each stage. The goal is to provide an analytic treatment of the circadian system, based on the three fundamental variables that are also represented in practically every model of the circadian clock, to obtain:

- an analytic periodic solution for the circadian system;
- a characterization of the cycle dynamics in terms of four fundamental threshold parameters;
- robustness of the circadian cycle, in terms of threshold parameters.

3.1 Model design

The first nonlinear term is the decreasing Hill function $V_R h^-(R)$ which can be simplified by a step function [15]. A straightforward choice for R_{int} is the threshold k_{Rr}, which gives:

$$V_R h^-(R) \approx \begin{cases} 0, & R > R_{int} \\ V_R, & R < R_{int} \end{cases} \tag{2}$$

The second nonlinear term is the common degradation of the complexes PER:CRY and CLOCK:BMAL1, $\gamma_B BP$, that goes through different well-marked steps as the oscillator performs one cycle. The same thresholds as for the cycle segmentation are used: B_{high}, P_{low} and P_{high}.

First, B remains close to its level B_{high} (whilst R and P are large) implying that the two terms $V_R h^-(R)$ and $\gamma_B BP$ have similar values and add up to 0 in the B equation, leading to the following simplification:

$$\gamma_B BP \approx \begin{cases} 0, & R > R_{int}, B < B_{high}, P_{low} < P < P_{high} \\ 0, & R > R_{int}, B < B_{high}, P > P_{high} \\ V_R, & R < R_{int}, B < B_{high}, P > P_{high} \end{cases} \tag{3}$$

These 3 equations correspond to the first three stages.

Next, we consider the dynamics between B and P. P decreases and tends to reach its low level P_{low}. B increases and so the degradation term is mostly dominated by B. The degradation term of B and P during stages 4 and 5 is then defined by:

$$\gamma_B BP \approx \begin{cases} \gamma_B BP_{low}, & R < R_{int}, B < B_{high}, P_{low} < P < P_{high} \\ \gamma_B BP_{low}, & R < R_{int}, B > B_{high}, P_{low} < P < P_{high} \end{cases} \tag{4}$$

At the end of stage 5, P reaches its low level P_{low} and B becomes close to a reference state B_{eq}, corresponding to the equilibrium between its production and degradation terms, $\dot{B} = V_R - \gamma_B B_{eq} P_{low} = 0$ which gives:

$$B_{eq} = \frac{V_R}{\gamma_B P_{low}}, \tag{5}$$

a relationship between B_{eq} and P_{low}.

Then, during stage 6, B reaches its maximum and P its minimum. We define the degradation term by a constant δ such that during stage 6 there is a time t where $\dot{P}(t) = 0$:

$$\gamma_B BP \approx \begin{cases} \gamma_B \delta, & R < R_{int}, B > B_{high}, P < P_{low} \end{cases} \tag{6}$$

The value δ stands for a product between a maximal B and a minimal P.

During stages 7 and 8, B decreases and tends to reach B_{eq} while P increases and crosses the threshold P_{low}. The degradation term is here described by:

$$\gamma_B BP \approx \begin{cases} \gamma_B B_{eq} P_{low}, & R > R_{int}, B > B_{high}, P < P_{low} \\ \gamma_B B_{eq} P_{low}, & R > R_{int}, B > B_{high}, P_{low} < P < P_{high} \end{cases} \tag{7}$$

Finally, to provide an initial starting point for the circadian cycle, we define the time at which the cycle exits stage i by t_i and the duration of each stage by the difference of exiting times:

$$d_i = t_i - t_{i-1} \text{ with } i = 1..8 \text{ and } t_0 = t_8 \tag{8}$$

We set the numerical starting point of the cycle as the point reached by the oscillator at the end of stage 5 (so $t_5 = 0$), when P crosses its threshold (so $P_0 = P_{low}$) and when the other variables B, D and R reach the value corresponding to an equlibrium between production and degradation rates, that is to say:

$$\begin{aligned} \text{End of stage 5} \Rightarrow P_0 &= P_{low} \\ \dot{B} = 0 \Rightarrow B_0 &= B_{eq} \\ \dot{D} = 0 \Rightarrow D_0 &= \frac{V_B B_{eq}}{\gamma_D} \\ \dot{R} = 0 \Rightarrow R_0 &= \frac{V_D V_B B_{eq}}{\gamma_D \gamma_R} \end{aligned} \tag{9}$$

In what follows, the point at the boundary between stages 5 and 6 (B_0, D_0, R_0, P_0) is the initial condition for the PWL system.

With these definitions, an analytical solution can be given for the dynamics of the model in each stage. Notice that these conditions and equations ensure positivity of B, D and R, provided that the threshold parameters are well-defined (see Section 3.2). As P reaches its minimum during stage 6, δ should also be defined carefully to ensure the positivity of P (in more detail below in Section 3.3). Table 1 summarizes the definitions of each stage, as well as the equations for each variable and the function trends expected to obtain oscillations and a consistent model, that is to say an oscillator that goes through all the stages in the specified physiological order.

3.2 Circadian cycle as a sequence of transitions between stages

The following assumptions and propositions summarize necessary conditions on the parameter values and on the stages durations, to ensure that the analytical solution represents an oscillator following the cycle transitions in the specified physiological order for one period (as defined in Section 2.3). Sketches of proofs are given in Appendix.

First, some assumptions among the parameters are as follows:

A.1 $\frac{V_R}{3\gamma_B} < \delta < \frac{V_R}{\gamma_B}$,

A.2 $B_{high} < B_{eq} = \frac{V_R}{\gamma_B P_{low}}$,

A.3 $P_{low} > \frac{2V_R}{3\delta\gamma_B - V_R}\frac{V_D V_B}{\gamma_D \gamma_B}$,

A.4 $\frac{V_D V_B V_R}{\gamma_D \gamma_R \gamma_B P_{low}} < R_{int} < \frac{V_R}{\gamma_R}$

Considering the requirements for the system to be in stage 6, Assumption A.1 ensures that B increases and remains above B_{high} and Assumption A.4 ensures the initial starting point R_0 lower than R_{int}. In addition to A.1 - A.4, the following assumptions on variables $D(t)$ and $R(t)$ are also needed. They are all verified by numerical results (see in Appendix Figure A1):

A.5 $\frac{V_B B_{eq}}{\gamma_D} < D_{min}$

A.6 $D(t_i) < \frac{V_R}{V_D}$, $i \in \{2, 3, 4, 5\}$.

A.7 $\frac{V_R}{V_D} < D(t_6) < D(t_7)$

A.8 $R_{int} < R(t_7) < R(t_8)$

The next propositions state the conditions needed at each step for transition from one stage to the next. At the starting point of the cycle, only the values of P_{low} and δ are set. Then, at each step, the idea is to define the value of a specific threshold by choosing the duration $d_i = t_i - t_{i-1}$ of stage i, such that the desired threshold is

crossed first. The duration d_i of stage i also depends on the duration d_{i-1} of stage $i-1$. These propositions ensure that Algorithm 1 returns a set of thresholds that guarantee a periodic cycle (see implementation in Section 3.3).

Since the starting point of the system occurs at the end of stage 5 (at t_5), the duration of stage 6 is the first one to be chosen. However, this duration directly impacts the good progress of the cycle, since a too short or too long duration blocks the beginning of the oscillations (see conditions of Proposition 1). Duration of stage 8 also requires precise conditions on the time intervals, to guarantee that the expected variable crosses its given threshold. Thus, for stages 6 and 8 (Propositions 1 and 2) an interval for the stage duration is provided, say $d_i \in (d_{i,min}, d_{i,max})$, to allow for flexibility in the threshold parameter choices.

Note that the transitions between two consecutive stages from stage 2 to 6 (see Proposition 4) follow naturally from the Assumptions A.1 - A.4 on model parameters only and from Propositions 1 to 3 and require no further conditions.

After one period, that is to say when the system reaches again the boundary between stage 5 and stage 6, $B(t_5) = B_0$ and $P(t_5) = P_0$. Indeed, during stage 5, B increases and converges quickly to $B_{eq} = B_0$ and the end of stage 5 corresponds to the moment where P equals P_{low} $(= P_0)$). Then, although $D(t_5)$ and $R(t_5)$ are observed bigger than D_0 and R_0, the good progress of the cycles of the next periods through the stages is not impacted.

Proposition 1 (Stage 6 to 7 to 8)**.** *Consider the PWL system as defined in Table 1. Assume that the following inequalities hold:*

1(i) $d_{6min} < d_6$ *such that* $D(t_5 + d_{6min}) > \frac{V_R}{V_D}$ *and* $\exists\ d_7 < \frac{(V_R - \delta\gamma_B)d_{6min}}{V_R}$ *such that* $P(t_5 + d_{6min} + d_7) = P_{low}$*;*

1(ii) $d_6 < d_{6max}$ *such that* $P(t_5 + d_{6max}) < P_{low}$ *and* $R(t_5 + d_{6max}) < \frac{V_R}{\gamma_R}$.

Then, starting at the boundary between stages 5 and 6 with initial condition (B_0, D_0, R_0, P_0) defined in Section 3.1, the system will successively cross stage 6 and enter stage 7 and cross stage 7 and enter stage 8.

Condition 1(i) ensures that P increases at the end of stage 6 and that d_6 is long enough to ensure a solution of the equation $P(t_6 + d_7) = P_{low}$, with d_7 such that P crosses P_{low}, before B crosses B_{high}. Condition 1(ii) ensures that R crosses R_{int} before P crosses P_{low}, and such that $R_{int} < \frac{V_R}{\gamma_R}$. These conditions guarantee transitions from stage 6 to 7 and from stage 7 to 8.

Proposition 2 (Stage 8 to 1)**.** *Consider the PWL system as defined in Table 1. In addition to the inequalities of Proposition 1, assume that the following inequalities hold :*

2(i) $d_{8min} < d_8 < d_{8max}$ *with* $d_{8min} = \frac{B(t_7) - \frac{V_R}{\gamma_B P_{low}}}{V_R}$ *and* $d_{8max} = \frac{B(t_7)}{V_R}$*;*

2(ii) $P(t_7 + d_{8max}) \ll P_{high}$.

Then, starting from stage 8, with initial conditions $B_0 = B(t_7)$, $D_0 = D(t_7)$, $R_0 = R(t_7)$, $P_0 = P(t_7) = P_{low}$, *the system will cross stage 8 and enter stage 1.*
Conditions 2(i) and 2(ii) ensure that B crosses B_{high} (such that $0 < B_{high} < B_{eq}$) before P crosses P_{high}, which guarantees transition from stage 8 to 1.

Proposition 3 (Stage 1 to 2)**.** *Consider the PWL system as defined in Table 1. In addition to the inequalities of Propositions 1 and 2, assume that the following inequality holds:*

3(i) $P_{high} < P(t_8 + d_{1max})$, *such that* $R(t_8 + d_{1max}) = R_{int}$.

Then, starting from stage 1, with initial conditions $B_0 = B(t_8) = B_{high}$, $D_0 = D(t_8)$, $R_0 = R(t_8)$, $P_0 = P(t_8)$, *the system will cross stage 1 and enter stage 2.*
Condition 3(i) ensures that P crosses P_{high} before R crosses R_{int}, which guarantees transition from stage 1 to 2.

Proposition 4 (Stage 2 to 6)**.** *Consider the PWL system as defined in Table 1. Assume that inequalities of Propositions 1-3 hold. Then, starting from stage 2, with initial conditions* $B_0 = B(t_1)$, $D_0 = D(t_1)$, $R_0 = R(t_1)$, $P_0 = P(t_1) = P_{high}$, *the system will cross stage 2 and successively evolve through stages 3, 4, 5 and finally 6, in this order.*

3.3 Algorithm for numerical estimation of circadian cycle threshold parameters

We use the conditions defined before in the propositions and propose Algorithm 1 to estimate the five-dimensional parameter space, composed of the four thresholds B_{high}, R_{int}, P_{low} and P_{high} and the scaling factor δ, such that any oscillator of the PWL model follows the specified physiological stages order for several periods. Both definitions and conditions of the system ensure positivity of B, D, and R but positivity of P has to be verified, so we add a condition in this sense (see steps 3 and 4 of Algorithm 1).

As input of Algorithm 1, we take the same parameters as the ones of the continuous model 1, except for γ_R. This parameter has a big impact on the period and allow us to adjust the period around 24h for a better coherence with biological clocks (the initial value of γ_R gave periods around 33h).

Table 1 Segmentation of the circadian time into twelve stages and equations describing the dynamics of the circadian clock in each of the biologically-consistent stages, with function trends expected.

Stage	1	2	3	4
Stages conditions	$R > R_{int}$ $B < B_{high}$ $P_{low} < P < P_{high}$	$R > R_{int}$ $B < B_{high}$ $P > P_{high}$	$R < R_{int}$ $B < B_{high}$ $P > P_{high}$	$R < R_{int}$ $B < B_{high}$ $P_{low} < P < P_{high}$
CLOCK:BMAL1 $\dot{B} =$	$\rightarrow$ 0	$\rightarrow$ 0	$\rightarrow$ 0	$\nearrow$ $V_R - \gamma_B B P_{low} > 0$
DBP $\dot{D} =$	$\searrow$ $V_B B - \gamma_D D < 0$	$\searrow$ $V_B B - \gamma_D D < 0$	$\searrow$ $V_B B - \gamma_D D < 0$	$\searrow$ $V_B B - \gamma_D D < 0$
REV $\dot{R} =$	$\nearrow$ or $\nearrow \searrow$ $V_D D - \gamma_R R$	$\nearrow \searrow$ or $\searrow$ $V_D D - \gamma_R R$	$\searrow$ $V_D D - \gamma_R R < 0$	$\searrow$ $V_D D - \gamma_R R < 0$
PER:CRY $\dot{P} =$	$\nearrow$ $V_D D > 0$	$\nearrow$ $V_D D > 0$	$\searrow$ $V_D D - V_R < 0$	$\searrow$ $V_D D - \gamma_B B P_{low} < 0$

Stage	5	6	7	8
Stages conditions	$R < R_{int}$ $B > B_{high}$ $P_{low} < P < P_{high}$	$R < R_{int}$ $B > B_{high}$ $P < P_{low}$	$R > R_{int}$ $B > B_{high}$ $P < P_{low}$	$R > R_{int}$ $B > B_{high}$ $P_{low} < P < P_{high}$
CLOCK:BMAL1 $\dot{B} =$	$\nearrow$ $V_R - \gamma_B B P_{low} > 0$	$\nearrow$ $V_R - \gamma_B \delta > 0$	$\searrow$ $-\gamma_B B_{eq} P_{low}$ $= -V_R < 0$	$\searrow$ $-\gamma_B B_{eq} P_{low}$ $= -V_R < 0$
DBP $\dot{D} =$	$\searrow$ $V_B B - \gamma_D D < 0$	$\nearrow$ $V_B B - \gamma_D D > 0$	$\nearrow$ or $\nearrow \searrow$ $V_B B - \gamma_D D$	$\nearrow \searrow$ or $\searrow$ $V_B B - \gamma_D D$
REV $\dot{R} =$	$\searrow$ $V_D D - \gamma_R R < 0$	$\nearrow$ $V_D D - \gamma_R R > 0$	$\nearrow$ $V_D D - \gamma_R R > 0$	$\nearrow$ $V_D D - \gamma_R R > 0$
PER:CRY $\dot{P} =$	$\searrow$ $V_D D - \gamma_B B P_{low} < 0$	$\searrow \nearrow$ $V_D D - \gamma_B \delta$	$\nearrow$ $V_D D - \gamma_B B_{eq} P_{low}$ $= V_D D - V_R > 0$	$\nearrow$ $V_D D - \gamma_B B_{eq} P_{low}$ $= V_D D - V_R > 0$

Stage	9 (stage refuted)	10 (stage refuted)	11 (stage refuted)	12 (stage refuted)
Stages conditions	$R < R_{int}$ $B < B_{high}$ $P < P_{low}$	$R > R_{int}$ $B < B_{high}$ $P < P_{low}$	$R < R_{int}$ $B > B_{high}$ $P > P_{high}$	$R > R_{int}$ $B > B_{high}$ $P > P_{high}$

Algorithm 1. Numerical estimation of the threshold parameters.

0. **Input:** $V_R = 44.4$, $k_{Rr} = 80.1$, $V_B = 0.142$, $V_D = 19$, $\gamma_R = 0.7$, $\gamma_D = 0.156$, $\gamma_B = 2.58$.

1. Pick δ such that $\frac{V_R}{3\gamma_B} < \delta < \frac{V_R}{\gamma_B}$.

2. Pick P_{low} such that $P_{low} > \frac{2V_R}{3\delta\gamma_B - V_R}\frac{V_D V_B}{\gamma_D \gamma_B}$, and define $B_{eq} = \frac{V_R}{\gamma_B P_{low}}$.

3. Compute $t_{P_{min}}$ solving $D(t_{P_{min}}) = \frac{\delta\gamma_B}{V_D}$.

4. Check:
   - if $P(t_{P_{min}}) > 0$ go to 5.
   - if $P(t_{P_{min}}) < 0$ go back to 1 and pick another δ.

5. Pick d_6 such that $d_{6min} < d_6 < d_{6max}$ with d_{6min} such that $D(t_5 + d_{6min}) > \frac{V_R}{V_D}$ and d_{6max} such that $P(t_5 + d_{6max}) < P_{low}$ and $R(t_5 + d_{6max}) < \frac{V_R}{\gamma_R}$

6. Compute d_7 such that $P(t_6 + d_7) = P_{low}$.

7. Check:
   - if $d_7 < \frac{(V_R - \delta\gamma_B)d_6}{V_R}$ go to 6.
   - if there is no solution or if $d_7 > \frac{(V_R - \delta\gamma_B)d_6}{V_R}$ go back to 3 and pick another d_6.

8. Compute R_{int} such that $R_{int} = R(t_5 + d_6)$.

9. Pick d_8 such that $\frac{B(t_7) - \frac{V_R}{\gamma_B P_{low}}}{V_R} < d_8 < \frac{B(t_7)}{V_R}$.

10. Compute B_{high} such that $B(t_7 + d_8) = B_{high}$.

11. Compute P_{high} such that $P(t_8) + p_{add} = P_{high}$, with $p_{add} = 200$ initially.

12. Compute d_{1max} such that $R(t8 + d_{1max}) = R_{int}$

13. Check:
   - if $P(t_8 + d_{1max}) > P_{high}$ go to 13.
   - if $P(t_8 + d_{1max}) < P_{high}$ go back to 10 with $p_{add} = p_{add} - 10$.

14. Check if the oscillator goes through all the eight stages in the specified physiological order for several periods and save the parameter values.

15. **Output:** set of parameters describing a circadian cycle: δ, P_{low}, R_{int}, B_{high}, P_{high}.

4 Continuous and PWL models share qualitative properties

Following the different steps of Algorithm 1, we estimate the five-dimensional parameter space by computing around 2000 combinations of values for the thresholds and δ (see Section 5.1 for more details). To better appreciate how the PWL approximates the continuous model (1), we compare the dynamics and characteristics of these two models.

4.1 Cycle oscillations

Figure 2(a) shows an example of an oscillator whose threshold values have been computed by Algorithm 1 while Figure 2(b) represents the oscillations of the continuous model. Notice that both models recover the main properties of circadian clock we are focusing on through this paper, that is to say the phase opposition between B and P and the order of protein peaks. As might be expected, the maximal and minimal amplitudes of each protein vary between the two model formalisms, with the maximal value of P increasing by a factor of 1.5 and the maximal value R decreasing by about the same factor, while maximal value of B remains similar (for the PWL oscillator compared to the continuous one). In any case, the order among amplitudes is maintained, as are the forms of the curves and their dynamics.

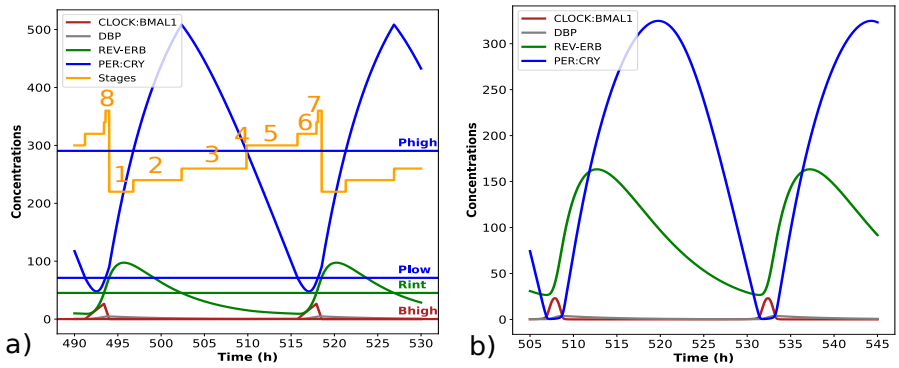

Fig. 2 Oscillations and cycle segmentation for (a) one oscillator generated by Algorithm 1 with δ =12.55, B_{high} =0.10, R_{int}=45.21, P_{low}=71.28 and P_{high}=290.55 and (b) for the continuous model (1).

4.2 Phase portraits

To go further in the analysis, we compare the phase portraits of the continuous model with those of several oscillators from the PWL model, with different parameters (see Figure 3).

Figure 3(a) highlights the phase opposition property, recovered by both models: when B reaches its highest values, P is low and inversely. Similarly, Figure 3(b) shows the similar dynamic between P and R, shared by all the oscillators: successively, R increases and reaches its highest values while P is at its intermediate ones, and then, as R decreases, P increases, peaks and decreases. From these figures, it is clear that the simplified PWL model closely represents the dynamical properties of the continuous model over a large range of its threshold parameters.

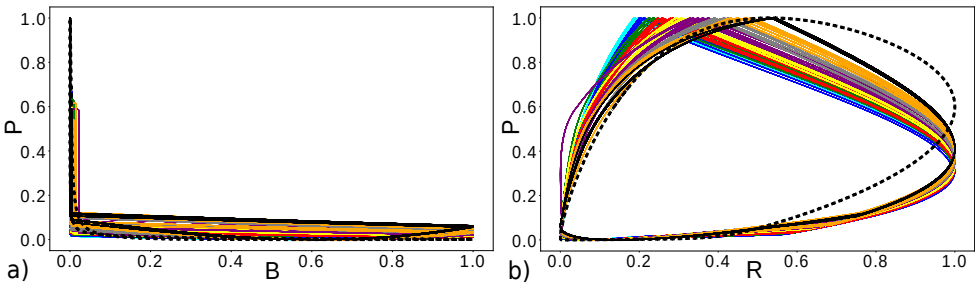

Fig. 3 Phase portrait projection on the planes: (a) B and P and (b) R and P for the continuous model (dashed black line) and for the PWL model (with different threshold parameters and one color stands for one δ value). Curves are normalized between 0 and 1 for comparison.

5 Cycle robustness: stage duration and critical elements

In this Section, we compare quantitatively the cycles obtained with the threshold parameters generated by Algorithm 1. We thus introduce the following elements which will next serve as comparative analysis tools between all the oscillators obtained. Letting $X \in \{B, R, P\}$, define:

1. A_{X_ϕ}: threshold values (called X_ϕ) relative to the amplitude $(X_{max} - X_{min})$ of the corresponding variables (X):

$$A_{X_\phi} = \frac{X_\phi - X_{min}}{X_{max} - X_{min}} \cdot 100 \tag{10}$$

2. τ_{X_ϕ}: time in hours that each variable (X) remains above its corresponding threshold (X_ϕ) over one period (T), corresponding also to protein peak duration:

$$\tau_{X_\phi} = \frac{t_{end} - t_{in}}{T}, \text{ such that } X(t) > X_\phi, \forall t \in [t_{in}, t_{end}] \tag{11}$$

3. d_i: stage duration:

$$d_i = t_i - t_{i-1}, \text{ with } i = 1..8 \text{ and } t_0 = t_8 \tag{12}$$

5.1 Parameter space

The parameter space of the PWL model is composed of the four threshold parameters: B_{high}, R_{int}, P_{low} and P_{high}, and of one scaling factor: δ. Figure 4 represents this five-dimensional parameter space as estimated by Algorithm 1 but, for a clearer comparison, the figure represents the relative amplitudes for each threshold parameter, as defined in equation (10).

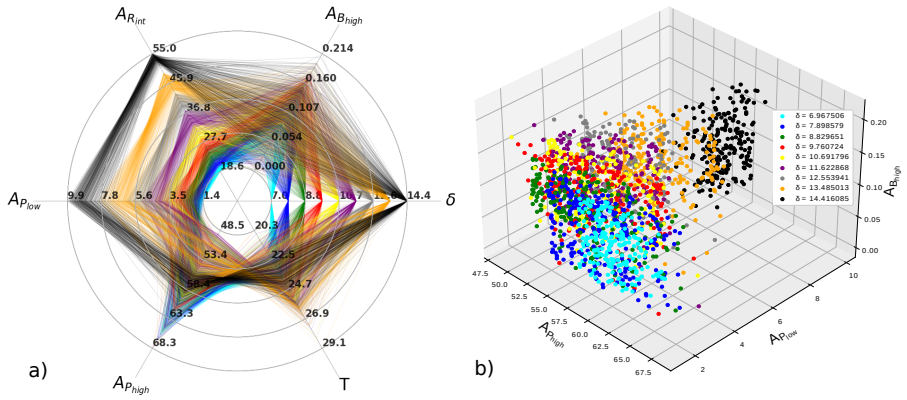

Fig. 4 (a),(b) Sets of threshold values computed by Algorithm 1 ensuring a correct representation of circadian clocks oscillations relatively to the amplitude of their corresponding variable (in %), and their associated period (T). One hexagon corresponds to one set of parameters. One color for each δ.

Thus, relatively to the amplitude of their corresponding variables, the values of R_{int}, P_{low} and P_{high} allowing the expected oscillations can be taken in a large range of concentrations. Notice nevertheless that $A_{R_{int}}$ and $A_{P_{low}}$ increase or decrease directly with δ while the relation between δ and $A_{P_{high}}$ is less clear. The way the system is constructed implies that the minimal value of B will always be close to B_{high} and thus $A_{B_{high}}$ is small.

Although the region of parameters values is wide, the periods (called T) of the oscillations of the PWL model remain in a small interval and are consistent with a circadian clock period, from 22 to 26h.

5.2 Timing expression of protein peaks

The definition of the PWL system provides a robust timing expression of protein peaks through all the oscillators, and for any parameters.

First, the variable B peaks when B is above its threshold B_{high} (during stages 5 to 8). More precisely, since during stage 6 B strictly increases ($\dot{B} = V_R - \gamma_B \delta > 0$ with Assumption A.1) and during stage 7 B strictly decreases ($\dot{B} = -V_R < 0$), B reaches its maximal value at the boundary between stage 6 and 7. During the rest of the cycle, B is closed to its minimal value, which is just below B_{high}.

At the opposite, P above P_{high} occurs during stages 2 and 3. The boundary between these two stages marks the point where P reaches its maximal value, with P strictly increasing during stage 2 ($\dot{P} = V_D D > 0$) and P strictly decreasing during stage 3 ($\dot{P} = V_D D - V_R < 0$ with Assumption A.6). P reaches its lowest values during stages 6 and 7, when P is below P_{low}. The system definition and Proposition 1 induce P minimal value during stage 6.

Finally, R maximal value is observed during stage 1, which is, as expected, between the peaks (highest values) of B and P.

5.3 Duration of protein peaks

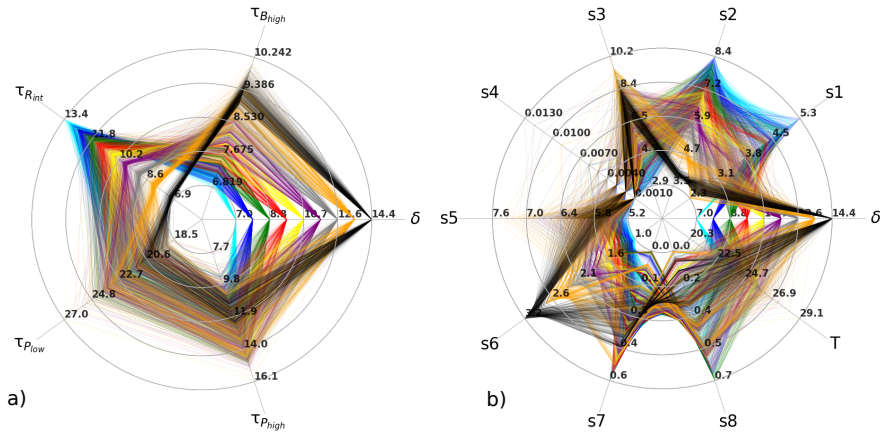

Fig. 5 Duration of protein peaks (a) and stages duration (b) in hours. One hexagon corresponds to one set of parameters. One color for each δ.

Figure 5(a) represents the peaks duration, as defined in equation (11), for each set of thresholds computed by Algorithm 1. Notice first that the duration of REV-ERB peak is inversely proportional to CLOCK:BMAL1 peak and to the scaling factor δ, highlighting one negative feedback loops characterizing circadian clocks: the more REV-ERB is expressed, the more CLOCK:BMAL1 is repressed, and inversely. The relation between $\tau_{B_{high}}$ and $\tau_{P_{high}}$ is less clear since the value of P_{high} is assessed last by Algorithm 1 and does not have a major influence on the correct progress of the cycle through the stages.

Then, the peak of B lasts between 7h and 10h and the peak of P lasts between 10h and 14h. The peak of R shows a larger range of durations, from 7 to 13h. Although no

constraint about protein peak durations were given, the durations of B and P peaks reasonably correspond to biological results [13]. Concerning R, the oscillators with the biggest δ ($\delta \gtrsim 11$) have a shorter peak of R (between 7 and 10h) and seem more consistent with biological results [16].

5.4 Duration of stages and relation to daylight/night intervals

As the circadian oscillator performs one cycle, it goes through well-marked steps highlighted by our stages. Figure 6 represents minimal and maximal values of stages durations after one period according to conditions from Propositions 1 to 4, while Figure 5(b) represent stages duration for the set of oscillators generated by Algorithm 1, after several periods.

As explained in Section 3.2, the duration of stage 6 is the first one to be defined, and directly depends on the values of δ and P_{low}. It varies from 1 to 3h and increases with δ and P_{low}. Then, stages 7 and 8 are very short and last less than one hour. Stage 8 marks the last moments before CLOCK:BMAL1 repression. The cycle enters stage 8 when P increases above its threshold P_{low} and reaches intermediates values. As soon as P increases, B is repressed suggesting that even intermediate values of P lead to a strong repression of the activity of B.

Duration of stages 1 and 2 evolve inversely with δ. During stage 1, which lasts from 2.5 to 5h, P progressively increases, repressing B while R is still expressed. Stage 2 lasts from 3.5 to 8h and a short stage 2 represents an earlier degradation of R compared to a long stage 2. Concerning stage 3, its duration seems to evolve similarly to δ, and goes from 3 to 8h.

Stage 4 is short and lasts less than half an hour. This stage corresponds to a weak expression of all the variables and the cycle enters stage 4 when P decreases under its threshold P_{high}, while R and B are low and leaves stage 4 when B increases above B_{high}. From a biological point of view, as soon as PER and CRY are degraded, CLOCK:BMAL1 is derepressed and starts its transcriptional activity. A short stage 4 could represent a fast derepression of B as soon as the levels of P are low and can be associated at the end of the poised state (see [13]).

Finally, duration of stage 5 is around 6 hours and stays consistent from an oscillator to another.

Next, we draw a closer comparison between our analytic stages and the experimental Circadian Time phases and establish a correspondence with daylight and night hours.

During daylight hours, from Circadian Time CT0 to CT12, both CLOCK:BMAL1 transcriptional activity and REV-ERB expression are observed, with a respective peak at approximately CT8 [13] and CT8-10 [13, 16–18].

In our segmentation, since the peak of B is represented by stages 5 to 8 (when $B > B_{high}$) and since we observed the peak of R during stage 1, we assume that daylight hours are represented by stages 5 to 1, with stage 1 marking the transition between daylight and night hours, around CT12. Night hours of Circadian Time (from CT12 to CT24) are characterized by high levels of PER:CRY, as described by stages 2 and 3 (with $P > P_{high}$) of our segmentation.

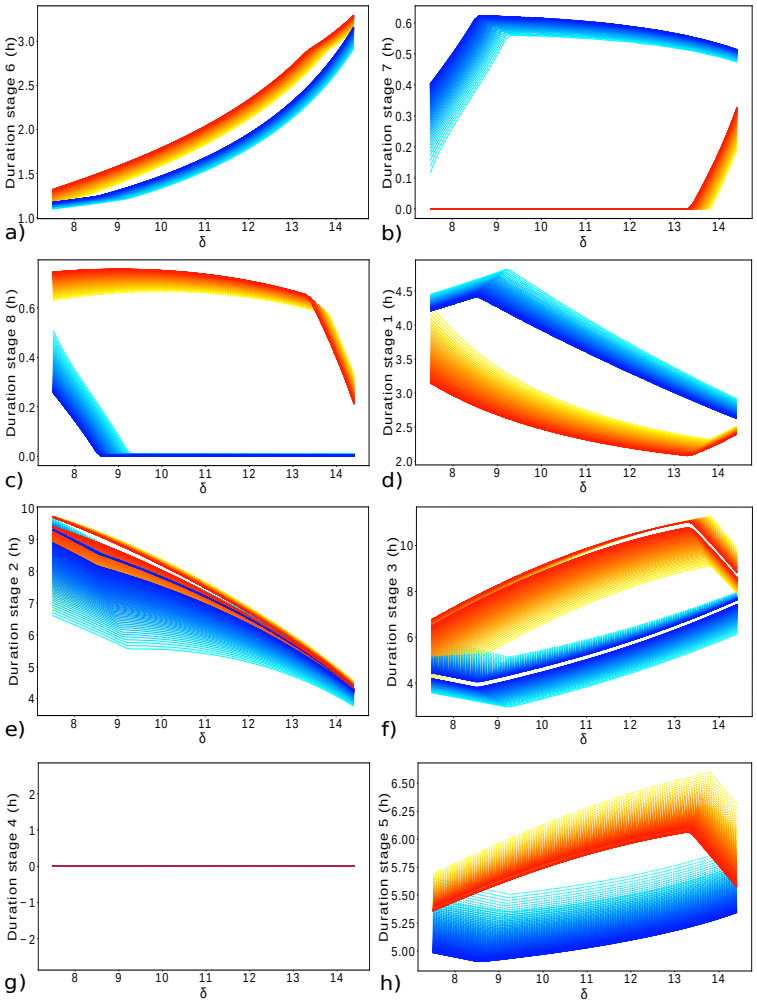

Fig. 6 (a) Minimal and maximal possible duration of stage 6 over δ according to conditions of Proposition 1 (lines in blue tones for $d6_{min}$ and in orange tones for $d6_{max}$). In each color, a darker line corresponds to a bigger P_{low}. (b) Durations of stage 7 over δ according to the minimal (lines in blue tones) and maximal (lines in orange tones) duration of stage 6. (c) Minimal and maximal possible duration of stage 8 over δ according to conditions of Proposition 2 (dashed lines for $d8_{min}$ and solid lines for $d8_{max}$) and according to the minimal and maximal duration of stage 6. (d-h) Durations of stages 1 to 5 are computed based on the minimal and maximal durations of stages 6 and 8. The lines use the same color and style code as for (a-c).

We can thus associate night hours to stages 2 and 3 and daylight hours to stages 4, 5, 6, 7, 8 and 1. In our model, night hours last around 10 to 14h and daylight hours are in a narrower interval, and are around 11-12h.

5.5 Two critical dynamical elements

Our analysis of stages duration and transitions identifies two critical moments during the circadian cycle: the first is the estimation of the duration of stage 6, where the system is defined by the scaling factor δ and which allows for P_{low} and R_{int} assessment, and the second is the evaluation of the duration of stage 8, which allows for B_{high} and P_{high} assessment.

In our piecewise linear model, the scaling factor δ represents the product of the concentrations PER:CRY and CLOCK:BMAL1, when they are in phase opposition with PER:CRY at its minimum value. In fact, during this interval, it is difficult to approximate the dynamics of the degradation term $\gamma_B BP$ by a linear term in the continuous model. The best (and simpler) option was to consider that the product is constant and equal to some δ for a suitable time interval. And, indeed, this value defines a kind of scaling of the cycle that directly impacts the first threshold parameters to be defined (P_{low} and R_{int}), varying them in direct proportion to δ (see Figure 4(a)).

It is interesting to note that, as the factor δ ranges over a large interval, it sets the scale for the other threshold parameters while keeping the total period close to 24 hour (in an interval between 22 and 26 hours).

Another critical point in the cycle appears at stage 8, when extra conditions on the crossing times of the variables B and P are needed to guarantee the correct order of transition (see Proposition 2). In fact, stage 8 marks the last moments before CLOCK:BMAL1 repression and is of short duration (less than 1h). P is at an intermediate value and increasing, and should effectively repress B before P itself crosses P_{high} (since P and B cannot be simultaneously above their highest thresholds). The variable R should wait for B repression before it also starts decreasing, which is verified by Assumption A.8. In other words, the dynamics at stage 8 potentially allows for different outcomes, so time control needs to be more strict in order to rule out the undesirable outcomes.

Globally, a well-defined duration of the stages 6-8 allow for a good assessment of all the parameters, ensuring the expected progress of the oscillator through the stages and sustained oscillations.

6 Discussion and conclusions

Our study is one of the first to propose a more precise, analytical and quantitative characterization of circadian clock cycle dynamics. In this perspective, we proposed a segmentation of the circadian cycle into eight stages based on the levels of expression of the core clock components CLOCK:BMAL1, REV-ERB and PER:CRY.

We first approximated a validated continuous model by piecewise linear (PWL) equations describing the dynamics of the circadian clock in each of these stages, in order to obtain an analytical characterization of the solutions. Thanks to the analytical results obtained with the PWL model, we proposed an Algorithm to compute, according to the scaling value δ, the region of parameters for the threshold values leading to circadian cycles in agreement with biological properties, and recovering the same qualitative dynamics as the continuous model of Almeida et al.

Our analysis shows that the PWL model allows for a large range of threshold parameters that exhibit the correctly ordered circadian cycle. An interesting feature of this model is the factor δ representing the product of the minimal concentration of PER:CRY and maximal of CLOCK:BMAL1. This parameter provides a scaling for the PWL model such that, for each value of δ, a corresponding set of threshold parameters exists, that generate an ordered circadian cycle with period around 24 hours. In this way, a large range of allowed concentrations is established for the PWL, supporting high robustness of the system based on an inverse proportionality between PER:CRY and CLOCK:BMAL1, $B = \frac{\delta}{\gamma_B P}$, as the maximal concentration of CLOCK:BMAL1 becomes high, the minimum of PER:CRY should become smaller.

Thus, among other quantitative points, our analysis indicates that the two concentrations minimal PER:CRY and maximal CLOCK:BMAL1 play a large role in setting the oscillatory regime of the cycle, and guarantee its robustness over a large range of concentrations.

To go further in our quantitative analysis, we plan to adapt our segmentation of the cycle to any circadian clock model built with ODEs and that includes the three main components B, R and P. This cycle partition will help characterize and compare circadian cycles quantitatively, notably to study mathematical model's agreement to biological properties, or highlight its most relevant terms for cycle robustness.

Acknowledgments. We thank Franck Delaunay for many enlightening discussions.

Declarations

- Funding. This work was supported in part by project InSync ANR-22-CE45-0012-01 and by LABEX SIGNALIFE (ANR-11-LABX-0028-01) from the program Investments for the Future of the French National Agency for Research.
- Availability of data and materials. This paper generates a new piecewise linear model which is based on a previously published ODE model (cited in the bibliography, and described in the text). An algorithm is then proposed to explore and characterize the parameter space of the new model. Numerical simulations of this algorithm generate the data analyzed in the paper. All parameters and conditions are provided to allow for computational reproduction of the data. The authors are planning to deposit the main codes in an appropriate repository.

Appendix A Proofs of Propositions 1 to 4 and illustration of Assumptions A.6-A.8

Proof of Proposition 1: Consider the system during stage 6, that is to say for $t_5 < t < t_6$. Since $\dot{B} = V_B - \gamma_B \delta$, Assumption A.1 implies that $B(t)$ strictly increases, so $B(t)$ remains higher than B_{high}.

Then, we can show that in $[t_5,t_6]$, $D(t)$ increases. Indeed, $\dot{D}(t) = V_B B(t) - \gamma_D D(t)$. Replacing $B(t)$ and $D(t)$ by their analytical solutions during stage 6, with initial

conditions $B_0 = B_{eq}$ and $D_0 = \frac{V_B B_{eq}}{\gamma_D}$,

$$\dot{D}(t) = \frac{V_B(V_R - \delta\gamma_B)}{\gamma_D}(1 - e^{-\gamma_D(t-t_5)}).$$

Assumption A.1 gives $\frac{V_B(V_R-\delta\gamma_B)}{\gamma_D} > 0$. Since $t - t_5 > 0$, $\dot{D}(t) > 0$ and $D(t)$ increases. Next, set $\sigma = \frac{V_D V_B(V_R-\gamma_B\delta)}{\gamma_D}$ and notice that,

$$\dot{R}(t) = V_D D(t) - \gamma_R R(t) = \frac{\sigma}{\gamma_D - \gamma_R}\left(e^{-\gamma_D(t-t_5)} - e^{-\gamma_R(t-t_5)}\right) + \frac{\sigma}{\gamma_R}\left(1 - e^{-\gamma_R(t-t_5)}\right)$$

$\forall t > t_5$, $\dot{R}(t) > 0$. Thus, $R(t)$ increases during stage 6.

Conditions A.1 and A.3 imply a decrease of $P(t)$ at the beginning of stage 6:

$$\dot{P}(t_5) = V_D D(t_5) - \delta\gamma_B = \frac{V_D V_B V_R}{\gamma_D \gamma_B P_{low}} - \delta\gamma_B < 0.$$

To guarantee that the system evolves to stage 7, it is necessary that $P(t)$ increases at the end of stage 6 and that $R(t)$ reaches R_{int} before $P(t)$ reaches P_{low}. This is assured by conditions 1(i) and 1(ii). The system enters stage 7.

Consider the system during stage 7, that is $t_6 < t < t_7$. Since $\dot{B}(t) = -V_R$ in this interval, $B(t)$ decreases according to the expression $B(t) = B(t_6) - V_R(t - t_6)$. By Assumption A.7, $D(t_6) > \frac{V_R}{V_D}$. At the beginning of stage 7 we have $R(t_6) = R_{int} < \frac{V_R}{\gamma_R}$ (by Assumption A.4). Then, for an interval $t \in (t_6, t_6 + o_7)$, with $o_7 > 0$ both $R(t)$ and $P(t)$ increase:

$$\begin{aligned}\dot{R}(t) &= V_D D(t) - \gamma_R R(t) > V_D \frac{V_R}{V_D} - \gamma_R R_{int} > 0\\ \dot{P}(t) &= V_D D(t) - V_R \approx V_D D(t_6) - V_R > 0.\end{aligned}$$

Now, we want to find a duration d_7 such that $P(t)$ crosses its threshold P_{low} before $B(t)$ decreases to B_{high}. To achieve this, set: $P(t_6 + d_7) = P_{low}$ and $B(t_6 + d_7) = B(t_6) - V_R d_7 > B_{high}$. Substituting for $B(t_6)$ and recalling that $B(t_5) = B_{high}$ obtains:

$$B(t_5) + (V_R - \gamma_B\delta)d_6 - B_{high} > V_R d_7 \;\Leftrightarrow\; d_7 < \frac{1}{V_R}(V_R - \gamma_B\delta)d_6$$

This last inequality holds by condition 1(i), ensuring that the system enters stage 8. □

Proof of Proposition 2: Consider the system during stage 8, that is $t_7 < t < t_8$. Since $\dot{B}(t) = -V_R$ in this interval, $B(t)$ decreases according to the expression $B(t) = B(t_7) - V_R(t - t_7)$. By assumption A.8, $R(t_8) > R_{int}$. By Assumption A.7, $D(t_7) > \frac{V_R}{V_D}$, which implies $\dot{P}(t_7) = V_D D(t_7) - V_R > 0$ and $P(t)$ increases in an interval $[t_7, t_7 + o_8)$, with $o_7 > 0$.

By condition 2(ii), $P(t_7 + d_{8max}) < P_{high}$. To check that B is the first variable to cross its threshold, compute the values of $B(t)$ at the instants t_7+d_{8min} and t_7+d_{8max}, as given by equalities 2(i):

$$\begin{aligned} B(t_7 + d_{8min}) &= B(t_7) - V_R(t_7 + d_{8min} - t_7) = B(t_7) - (B(t_7) - B_{eq}) = B_{eq}, \\ B(t_7 + d_{8max}) &= B(t_7) - V_R(t_7 + d_{8max} - t_7) = B(t_7) - B(t_7) = 0, \end{aligned}$$

and recall that $B_{eq} > B_{high}$. So, since $B(t)$ is continuous, there exists some d_8 with $d_{8min} < d_8 < d_{8max}$, such that $B(t_7 + d_8) = B_{high}$. The system enters stage 1. □

Proof of Proposition 3: Consider the system during stage 1, that is $t_8 < t < t_1$. During this interval, $\dot{B}(t) = 0$, implying that $B(t)$ remains constant. Since $B(t)$ enters stage 1 as $B(t)$ crosses below B_{high}, we can write $B(t) \approx B_{high}$.

The equation for P is $\dot{P}(t) = V_D D(t) > 0$ implying that $P(t)$ increases. Then, condition 3(i) implies that $P(t)$ will cross its threshold P_{high} before $R(t)$ crosses R_{int}. The system enters stage 2. □

Proof of Proposition 4: In $[t_8,t_3]$, $\dot{B}(t) = 0$ implies that $B(t)$ is constant, with $B(t) \approx B_{high}$. While $B(t)$ is constant, $D(t)$ satisfies $\dot{D}(t) = V_B B_{high} - \gamma_D D(t)$ and has the form:

$$D(t) = \left(D(t_8) - \frac{V_B B_{high}}{\gamma_D} \right) e^{-\gamma_D (t - t_8)} + \frac{V_B B_{high}}{\gamma_D}. \tag{A1}$$

Since $D_{min} > \frac{V_B B_{eq}}{\gamma_D} > \frac{V_B B_{high}}{\gamma_D}$ (by Assumption A.5), $D(t)$ decreases and approaches D_{min} as t increases. Eventually, $R(t)$ also decreases for $t < t_3$ and approaches $R(t_3) = \frac{V_D V_B B_{high}}{\gamma_R \gamma_D}$.

In $[t_1, t_2]$, $\dot{P}(t) = V_D D(t) > 0$ implies that $P(t)$ increases and will remain above P_{high}. Therefore, the next variable to cross a threshold is $R(t)$, it decreases and will reach $R(t_2) = R_{int}$, so the system enters stage 3.

In $[t_2, t_3]$, $D(t_2) < \frac{V_R}{V_D}$ by Assumption A.6, and $D(t)$ is still decreasing. Now this implies $\dot{P} = V_D D - V_R < 0$, so P decreases until it crosses $P_{high} = P(t_3)$, and the system enters stage 4.

Consider next the system during stage 4, that is to say $t_3 < t < t_4$. As the oscillator enters stage 4, $B(t_3) \lesssim B_{high}$, $R(t_3) \ll R_{int}$ and $P(t_3) = P_{high}$.

Since $B_{high} < B_{eq} = \frac{V_R}{\gamma_B P_{low}}$ (see Assumption A.2), in an interval $[t_3, t_3 + o_4]$, with $o_4 > 0$, $B(t)$ will increase since $\dot{B}(t) = V_R - \gamma_B B(t) P_{low} > 0$. But, notice that $B(t_3) \lesssim B_{high}$ at the end of stage 3, which implies that $B(t_3 + \varepsilon) > B_{high}$ for any $\varepsilon > 0$. Therefore, $B(t)$ will cross its threshold with $B(t_4) = B_{high}$, the system enters stage 5, and $d_4 = t_4 - t_3$ is necessarily a very short interval.

Finally, consider the system during stage 5, that is to say $t_4 < t < t_5$. For $t_8 < t < t_4$ we had $B(t) \approx B_{high}$ so, at the beginning of stage 5, B satisfies $\dot{B}(t) =$

$V_R - \gamma_B B(t) P_{low} > 0$. $B(t)$ increases and converges quickly to B_{eq}. Thus, we can write $B(t) \approx B_{eq}$ during stage 5.

On some interval $[t_4, t_4 + o_5)$, with $o_5 > 0$ both $D(t)$ and $R(t)$ continue to decrease, as indicated by equation (A1). Namely $R(t) < R_{int}$.

In stage 5, $P(t)$ is governed by the equation $\dot{P}(t) = V_D D(t) - \gamma_B B(t) P_{low}$. By Assumption A.6, during stage 4 and 5, $D(t) < \frac{V_R}{V_D}$. $\dot{P}(t) \approx V_D D(t) - \gamma_B B_{eq} P_{low} \approx V_D D(t) - V_R < 0$ P decreases until it crosses P_{low} at $P(t_5)$, defining the entry of the system into stage 6. □

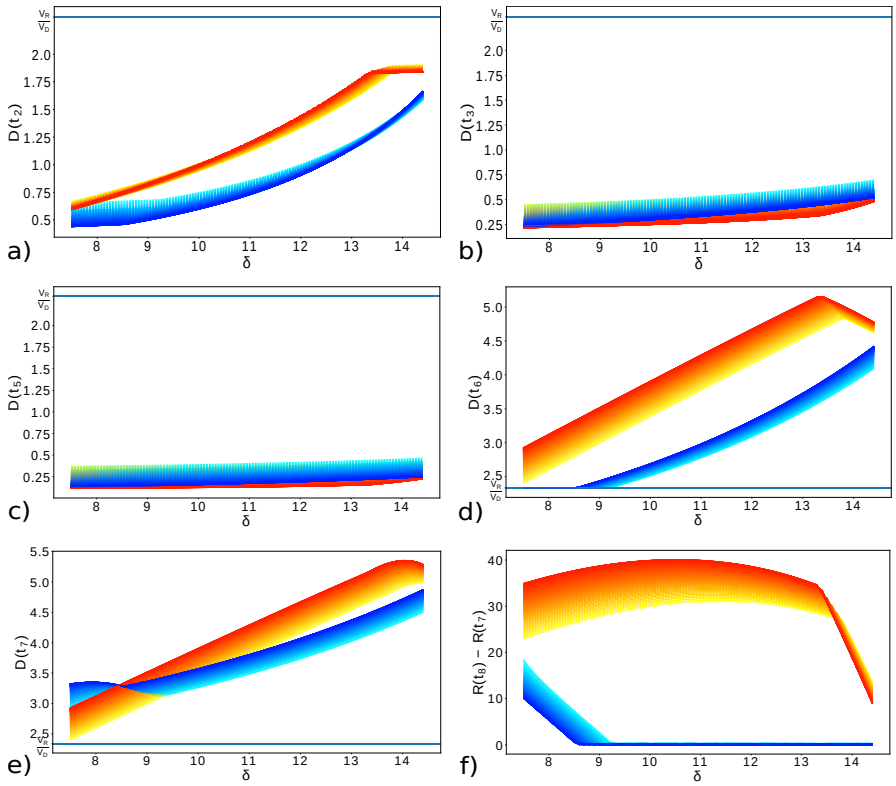

Fig. A1 Numerical simulations justifying Assumptions A.6-A.8 (see Section 3.2). (a-e) Values of $D(t_i)$, $i \in \{2, 3, 5, 6, 7\}$ to compare with $\frac{V_R}{V_D}$: illustration of Assumptions A.6 and A.7. (f) $R(t_8) - R(t_7)$ to compare with 0 : illustration of Assumption A.8. Each ending stage value depends on δ, P_{low} (a darker line corresponds to a bigger P_{low}), the duration of stage 6 (lines in blue tones for $d_{6_{min}}$ and in orange tones for $d_{6_{max}}$) and the duration of stage 8 (dashed lines for $d_{8_{min}}$ and solid lines for $d_{8_{max}}$). See caption of Figure 6 for more details.

References

[1] Koike, N., Yoo, S.-H., Huang, H.-C., Kumar, V., Lee, C., Kim, T.-K., Takahashi, J.S.: Transcriptional architecture and chromatin landscape of the core circadian clock in mammals. science **338**(6105), 349–354 (2012)

[2] Almeida, S., Chaves, M., Delaunay, F.: Transcription-based circadian mechanism controls the duration of molecular clock states in response to signaling inputs. Journal of theoretical biology **484**, 110015 (2020)

[3] Forger, D.B., Peskin, C.S.: A detailed predictive model of the mammalian circadian clock. Proceedings of the National Academy of Sciences **100**(25), 14806–14811 (2003)

[4] Relógio, A., Westermark, P.O., Wallach, T., Schellenberg, K., Kramer, A., Herzel, H.: Tuning the mammalian circadian clock: robust synergy of two loops. PLoS computational biology **7**(12), 1002309 (2011)

[5] Woller, A., Duez, H., Staels, B., Lefranc, M.: A mathematical model of the liver circadian clock linking feeding and fasting cycles to clock function. Cell reports **17**(4), 1087–1097 (2016)

[6] Korenčič, A., Bordyugov, G., Košir, R., Rozman, D., Goličnik, M., Herzel, H.: The interplay of cis-regulatory elements rules circadian rhythms in mouse liver. PloS one **7**(11), 46835 (2012)

[7] Hesse, J., Martinelli, J., Aboumanify, O., Ballesta, A., Relógio, A.: A mathematical model of the circadian clock and drug pharmacology to optimize irinotecan administration timing in colorectal cancer. Computational and Structural Biotechnology Journal **19**, 5170–5183 (2021)

[8] Woller, A., Gonze, D.: Modeling clock-related metabolic syndrome due to conflicting light and food cues. Scientific reports **8**(1), 1–10 (2018)

[9] Brown, L.S., Doyle III, F.J.: A dual-feedback loop model of the mammalian circadian clock for multi-input control of circadian phase. PLoS Computational Biology **16**(11), 1008459 (2020)

[10] Gonze, D., Halloy, J., Goldbeter, A.: Robustness of circadian rhythms with respect to molecular noise. Proceedings of the National Academy of Sciences **99**(2), 673–678 (2002)

[11] Almeida, S., Chaves, M., Delaunay, F.: Control of synchronization ratios in clock-/cell cycle coupling by growth factors and glucocorticoids. Royal Society Open Science **7**(2), 192054 (2020)

[12] Feillet, C., Krusche, P., Tamanini, F., Janssens, R.C., Downey, M.J., Martin, P., Teboul, M., Saito, S., Lévi, F.A., Bretschneider, T., *et al.*: Phase locking and

multiple oscillating attractors for the coupled mammalian clock and cell cycle. Proceedings of the National Academy of Sciences **111**(27), 9828–9833 (2014)

[13] Takahashi, J.S.: Transcriptional architecture of the mammalian circadian clock. Nature Reviews Genetics **18**(3), 164–179 (2017)

[14] Burckard, O., Teboul, M., Delaunay, F., Chaves, M.: Cycle dynamics and synchronization in a coupled network of peripheral circadian clocks. Interface Focus **12**(3), 20210087 (2022)

[15] Casey, R., Jong, H.d., Gouzé, J.-L.: Piecewise-linear models of genetic regulatory networks: equilibria and their stability. Journal of mathematical biology **52**(1), 27–56 (2006)

[16] Bugge, A., Feng, D., Everett, L.J., Briggs, E.R., Mullican, S.E., Wang, F., Jager, J., Lazar, M.A.: Rev-erbα and rev-erbβ coordinately protect the circadian clock and normal metabolic function. Genes & development **26**(7), 657–667 (2012)

[17] Feng, D., Liu, T., Sun, Z., Bugge, A., Mullican, S.E., Alenghat, T., Liu, X.S., Lazar, M.A.: A circadian rhythm orchestrated by histone deacetylase 3 controls hepatic lipid metabolism. Science **331**(6022), 1315–1319 (2011)

[18] Cho, H., Zhao, X., Hatori, M., Yu, R.T., Barish, G.D., Lam, M.T., Chong, L.-W., DiTacchio, L., Atkins, A.R., Glass, C.K., *et al.*: Regulation of circadian behaviour and metabolism by rev-erb-α and rev-erb-β. Nature **485**(7396), 123–127 (2012)